

# Transport model study of transverse momentum distributions of Pion, kaon, and (anti-)proton production in U+U collisions at

$$\sqrt{s_{NN}} = 193 \text{ GeV}$$

Ying Yuan,<sup>1,2\*</sup>

1) *College of Pharmacy,*

*Guangxi University of Chinese Medicine,*

*Nanning 530200, China*

2) *Guangxi Key Laboratory of Nuclear Physics and Nuclear Technology,*

*Guangxi Normal University,*

*Guilin 541004, China*

## Abstract

The transverse momentum spectra of  $\pi^\pm$ ,  $k^\pm$  and  $p(\bar{p})$  in midrapidity ( $|y| < 0.1$ ) for nine centrality classes : 0 – 5%, 5 – 10%, 10 – 20%, 20 – 30%, 30 – 40%, 40 – 50%, 50 – 60%, 60 – 70% and 70 – 80% in  $^{238}\text{U}+^{238}\text{U}$  collisions at  $\sqrt{s_{NN}}=193$  GeV are studied within the framework of the cascade and soft momentum dependent equation of state (SM-EoS) mode of the UrQMD model. Other extracted observables from  $p_T$  spectra such as average transverse momentum ( $\langle p_T \rangle$ ), particle yields ( $dN/dy$ ) and particle ratios are also shown as functions of collision centrality. It is found that the U+U collision process is segmented. Before the collision centrality is 50 – 60%, the experimental data are described well using cascade mode when the  $p_T < 1.2\text{GeV}/c$ . The results are in good agreement with the experimental data using the SM-EoS mode at  $p_T > 1.2\text{GeV}/c$ . For the case of 60 – 80% centrality, the SM-EoS mode describes the data better. Anti-particle to particle yield ratios indicating pair production is the dominant mechanism of particle production at RHIC energy.

PACS numbers: 24.10.Lx, 25.75.Dw, 25.75.-q

Keywords: UrQMD model; cascade; SM-EoS; transverse momentum distributions; U+U collisions

---

\* E-mail address: yuany@gxtnmu.edu.cn

## I. INTRODUCTION

Heavy ion collisions (HICs) at super-relativistic energies provide an excellent opportunity to explore the properties of strongly interacting matter at extreme temperatures and densities<sup>[1–7]</sup>. The mechanism of particles and fragments generation in super-relativistic HICs deserves further investigation, as it may provide important information about the quantum chromodynamics (QCD) phase transition from quark-gluon plasma (QGP) to hadron gas (HG).<sup>[8, 9]</sup>. Over the past two decades, many experiments have been conducted at the Relativistic Heavy Ion Collider (RHIC) near the critical energy of the hadronic matter to QGP phase transition.<sup>[10]</sup>. Theoretical studies on particle and antiparticle generation have been carried out for many years, such as statistical model, coalescence model and transport model<sup>[11–19]</sup>. The investigation of transport phenomena is particularly crucial in comprehending numerous fundamental properties<sup>[20]</sup>. The transverse momentum spectra of particles produced in high-energy collisions are of high study value because they can provide us with critical information about the frozen state of the dynamics of interacting systems<sup>[21]</sup>. Experiments carried out at the Relativistic Heavy Ion Collider (RHIC) have shown that in a U+U collision with a center of mass energy of 193 GeV, a very dense medium consisting of defined quarks and gluons is formed<sup>[22]</sup>.

In this paper, the Ultra-relativistic Quantum Molecular Dynamics (UrQMD) transport model is adopted to produce the transverse momentum distributions of  $\pi$  mesons,  $k$  mesons and  $p(\bar{p})$  in U+U collisions at  $\sqrt{s_{NN}}=193$  GeV including nuclear collision in all directions, and compared with experimental data taken from the STAR Collaboration<sup>[23]</sup>. The main aim of this work is to extract information about nuclear reactions, such as the effect of the initial geometry of the collided nuclei on the final state particle generation in U+U collisions at RHIC energies.

## II. ULTRARELATIVISTIC QUANTUM MOLECULAR DYNAMICS TRANSPORT MODEL

### A. The UrQMD model

The UrQMD model is a microscopic many-body transport approach and can be applied to study proton-proton (pp), proton-nucleus (pA) and nucleus-nucleus (AA) interactions

over an energy range from the SIS to LHC. This transport model is based on the covariant propagation of color strings, constituent quarks and diquarks (as string ends) accompanied by mesonic and baryonic degree of freedom<sup>[24]</sup>. It can combine different reaction mechanisms and give theoretical simulation results of various experimental observations. In the present model, the subhadronic degrees of freedom enter via the introduction of a formation time for hadrons produced in the fragmentation of strings<sup>[25–27]</sup>, which are dominant at the early stage of heavy ion collisions (HICs) with high SPS and RHIC energies.

The UrQMD model is based on parallel principles as the quantum molecular dynamics (QMD) model: hadrons are represented by Gaussian wave packets in phase space and the phase space of hadron  $i$  is propagated according to Hamilton's equation of motion<sup>[28]</sup>,

$$\dot{\vec{r}}_i = \frac{\partial H}{\partial \vec{p}_i}, \quad \dot{\vec{p}}_i = -\frac{\partial H}{\partial \vec{r}_i}. \quad (1)$$

Here,  $\vec{r}_i$  and  $\vec{p}_i$  are the coordinate and momentum of the hadron  $i$ , respectively. The Hamiltonian  $H$  consists of the kinetic energy  $T$  and the effective interaction potential energy  $U$ ,

$$H = T + U. \quad (2)$$

This microscopic transport approach simulates multiple interactions of in-going and newly produced particles, the excitation and fragmentation of color strings and the formation and decay of hadronic resonances. In the pursuit of higher energies, it is crucial to consider the treatment of subhadronic degrees of freedom. In the present model, these degrees of freedom enter via the introduction of a formation time for hadrons produced in the fragmentation of strings. A phase transition to a quark-gluon state is not incorporated explicitly into the model dynamics. However, a detailed analysis of the model in equilibrium, yields an effective equation of state of Hagedorn type<sup>[29]</sup>.

### **B. The soft momentum dependent equation of state (SM-EoS)**

In the standard UrQMD model, the potential energy  $U$  includes the two-body and three-body Skyrme-, Yukawa-, Coulomb- and Pauli-terms<sup>[30, 31]</sup>,

$$U = U_{\text{sky}}^{(2)} + U_{\text{sky}}^{(3)} + U_{\text{Yuk}} + U_{\text{Cou}} + U_{\text{pau}}. \quad (3)$$

In the modified version of UrQMD (based on the version 3.4), the following two terms are further added: (1) the density dependent symmetry potential term  $U_{\text{sym}}$  and (2) the

momentum-dependent term  $U_{\text{md}}$ <sup>[32]</sup>. In this work, the soft momentum dependent (SM) equation of state (EoS) are used, which is described in Ref. [33]. At the RHIC energy region, the Yukawa-, Pauli- and symmetry-potentials of baryons become negligible, while the Skyrme- and the momentum-dependent parts of potentials still influence the whole dynamical process of HICs<sup>[34]</sup>. During the formation time, the "pre-formed" particles (string fragments that will be projected onto hadron states later on) are usually treated to be free streaming, while reduced cross sections are only included for leading hadrons.

In this paper, the transverse momentum distributions and central yields of  $\pi$  mesons,  $k$  mesons and  $p(\bar{p})$  generated in U+U collisions at  $\sqrt{s_{NN}}=193$  GeV at mid-rapidity ( $|y|<0.1$ ) are studied by using UrQMD cascade mode and SM-EoS mode.

### III. RESULTS AND DISCUSSIONS

#### A. Transverse momentum spectra

Fig. 1 and Fig. 2 are shown the transverse momentum spectra in nine centrality classes in U+U collisions at  $\sqrt{s_{NN}}=193$  GeV at mid-rapidity ( $|y|<0.1$ ) for  $\pi^+$  and  $\pi^-$ . The nine different centrality classes are 0 – 5%, 5 – 10%, 10 – 20%, 20 – 30%, 30 – 40%, 40 – 50%, 50 – 60%, 60 – 70% and 70 – 80% respectively. The dotted lines are the results calculated from the cascade mode of UrQMD model. The solid lines are the results calculated from the soft momentum dependent equation of state mode of UrQMD model. The symbols are the experimental data from the STAR Collaboration<sup>[23]</sup>. The calculations are shown for  $p_T < 2.0\text{GeV}/c$  in the Figure (a) and (b). Figure (c) shows the results of the calculation for  $p_T < 1.2\text{GeV}/c$  taking into account the same systematic uncertainties as the experiment. It can be found that the cascade mode of UrQMD model can describe the experimental laws very well before 50 – 60% centrality. But the yield is higher than the experimental values in the central transverse momentum region. At 60 – 80% centrality, the SM-EoS mode can better describe the experimental results. When the uncertainty of the system is considered, the agreement with the experiment is better in Figure (c). In the region with  $1.2\text{GeV}/c < p_T < 2.0\text{GeV}/c$ , the cascade model can well describe the experimental data.

Fig. 3 and Fig. 4 are shown the transverse momentum spectra in nine centrality classes in U+U collisions at  $\sqrt{s_{NN}}=193$  GeV at mid-rapidity ( $|y|<0.1$ ) for  $k^+$  and  $k^-$ . The dotted

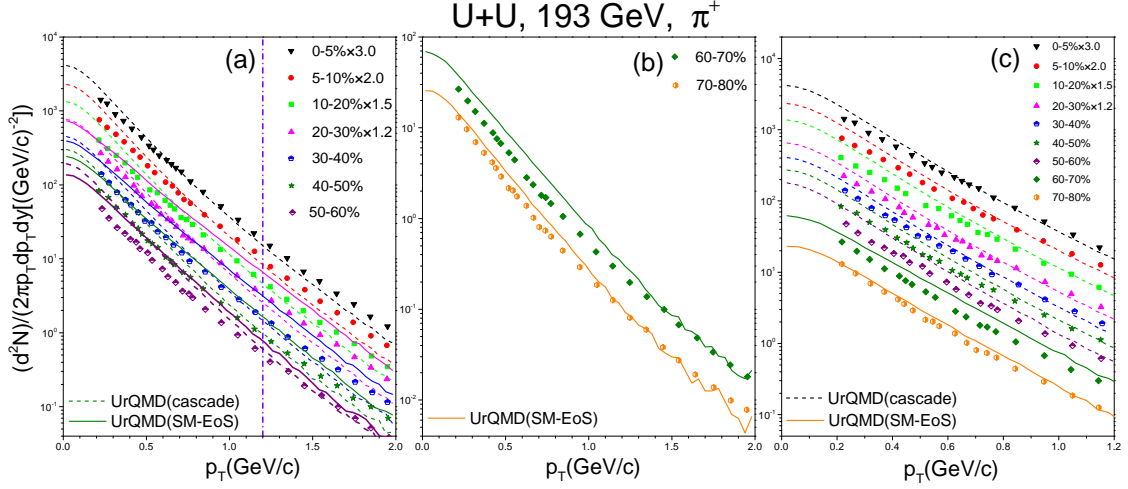


FIG. 1: Transverse momentum spectra of  $\pi^+$  are calculated at midrapidity ( $|y| < 0.1$ ) in U+U collisions at  $\sqrt{s_{NN}}=193$  GeV for 0–5%, 5–10%, 10–20%, 20–30%, 30–40%, 40–50%, 50–60%, 60–70% and 70–80% centralities from the cascade mode and the soft momentum dependent equation of state mode of UrQMD model. Calculations are shown by the lines. Experimental data taken from the STAR Collaboration<sup>[23]</sup> are represented by the symbols.

lines are the results calculated from the cascade mode of UrQMD model. The solid lines are the results calculated from the soft momentum dependent equation of state mode of UrQMD model. The symbols are the experimental data from the STAR Collaboration<sup>[23]</sup>. The calculations are shown for  $p_T < 2.0 \text{ GeV}/c$  in the Figure (a) and (b). Figure (c) shows the results of the calculation for  $p_T < 1.2 \text{ GeV}/c$  taking into account the same systematic uncertainties as the experiment. It can be found that the SM-EoS mode of UrQMD model can describe the overall change trend well, but it is about 1.6 times larger than the experimental result before 50–60% centrality in the region with  $p_T < 1.2 \text{ GeV}/c$ . With the increase of collision centrality, in the region, with  $p_T > 1.2 \text{ GeV}/c$ , the theoretical results are more and more consistent with the experimental results. At 60–80% centrality, the SM-EoS mode can better describe the experimental results. When the uncertainty of the system is considered, the yield is higher than the experimental values in the central

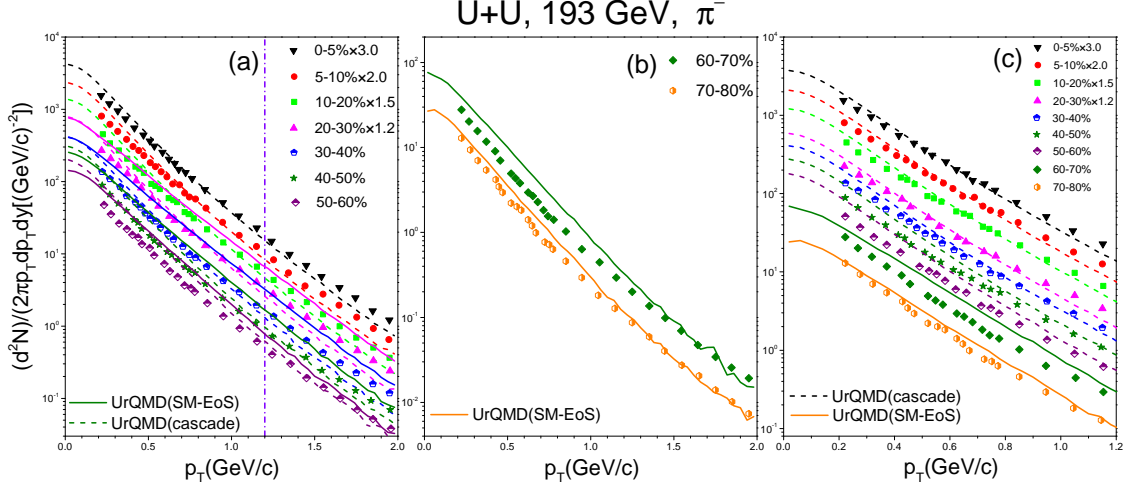


FIG. 2: Transverse momentum spectra of  $\pi^-$  are calculated at midrapidity ( $|y| < 0.1$ ) in U+U collisions at  $\sqrt{s_{NN}}=193$  GeV for 0–5%, 5–10%, 10–20%, 20–30%, 30–40%, 40–50%, 50–60%, 60–70% and 70–80% centralities from the cascade mode and the soft momentum dependent equation of state mode of UrQMD model. Calculations are shown by the lines. Experimental data taken from the STAR Collaboration<sup>[23]</sup> are represented by the symbols.

transverse momentum region in Figure (c).

Fig. 5 and Fig. 6 are shown the transverse momentum spectra in nine centrality classes in U+U collisions at  $\sqrt{s_{NN}}=193$  GeV at mid-rapidity ( $|y|<0.1$ ) for  $p$  and  $\bar{p}$ . The dotted lines are the results calculated from the cascade mode of UrQMD model. The solid lines are the results calculated from the soft momentum dependent equation of state mode of UrQMD model. The symbols are the experimental data from the STAR Collaboration<sup>[23]</sup>. The calculations are shown for  $p_T < 2.0\text{GeV}/c$  in the Figure (a) and (b). Figure (c) shows the results of the calculation for  $p_T < 1.2\text{GeV}/c$  taking into account the same systematic uncertainties as the experiment. It can be found that the cascade mode of UrQMD model can describe in good agreement with the experimental data for  $p_T < 1.2\text{GeV}/c$ , and the results are in good agreement with the experimental data under the SM-EoS mode in the region with  $1.2\text{GeV}/c < p_T < 2.0\text{GeV}/c$  before 50–60% centrality. With the increase of collision centrality, in the region with  $p_T > 1.2\text{GeV}/c$ , the theoretical results are more and

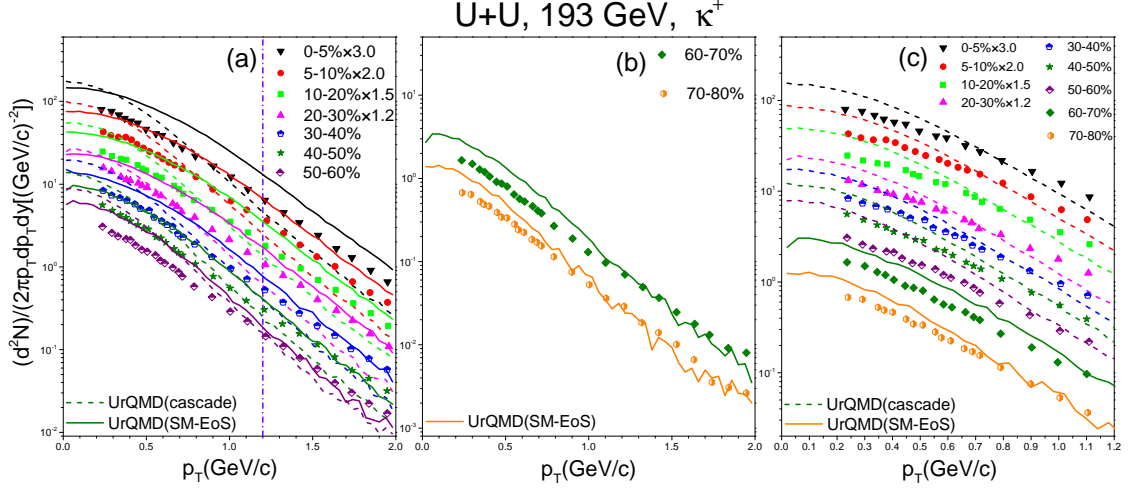


FIG. 3: Transverse momentum spectra of  $k^+$  are calculated at midrapidity ( $|y| < 0.1$ ) in U+U collisions at  $\sqrt{s_{NN}}=193$  GeV for 0–5%, 5–10%, 10–20%, 20–30%, 30–40%, 40–50%, 50–60%, 60–70% and 70–80% centralities from the cascade mode and the soft momentum dependent equation of state mode of UrQMD model. Calculations are shown by the lines. Experimental data taken from the STAR Collaboration<sup>[23]</sup> are represented by the symbols.

more consistent with the experimental results. At 60–80% centrality, the SM-EoS mode can better describe the experimental results. When the uncertainty of the system is considered, the yield is in good agreement with the experimental data in Figure (c).

In general, in the area of  $p_T < 1.2 \text{ GeV}/c$ , the cascade mode can better describe the experimental results. In the  $1.2 \text{ GeV}/c < p_T < 2.0 \text{ GeV}/c$  region, the SM-EoS model can better describe the experimental results. Here we describe the collision process of U+U in a piecewise way, because the Uranium nucleus is ellipsoidal, but we do not consider its deformation characteristics in the actual calculation, and think that the collision probability of the tip-tip, body-body and body-tip is the same. We will analyze the impact of the deformation in more detail in the future. As can be seen from Figure 1-6, the energy density in the central region is relatively large at the initial stage of collision, and the particles generated cannot fly away from the central region quickly, and they deposit part or all of their energy in the central region, so the effect of the equation of state is not important. As time goes on, the previously created particles interact with other nucleons and continue to

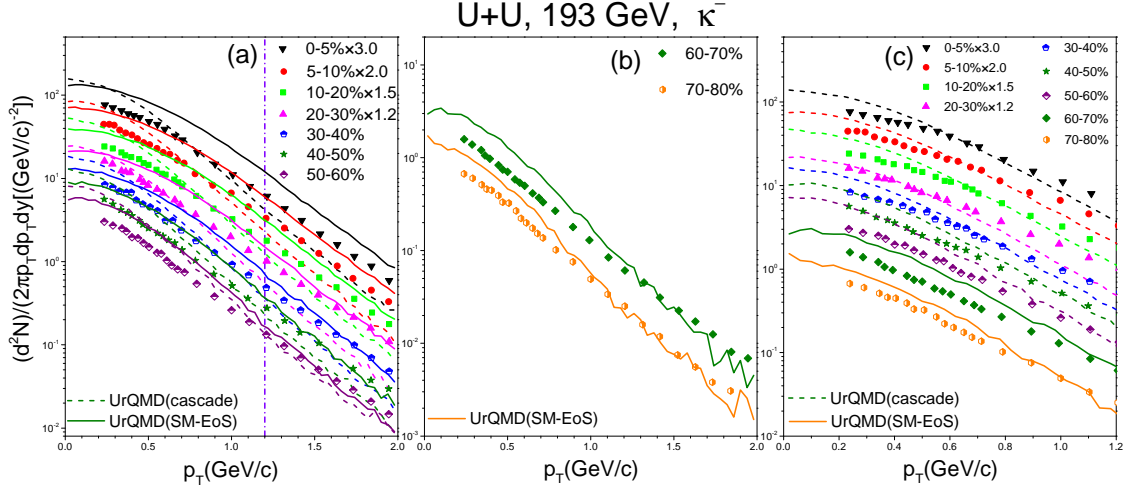


FIG. 4: Transverse momentum spectra of  $k^-$  are calculated at midrapidity ( $|y| < 0.1$ ) in U+U collisions at  $\sqrt{s_{NN}}=193$  GeV for 0–5%, 5–10%, 10–20%, 20–30%, 30–40%, 40–50%, 50–60%, 60–70% and 70–80% centralities from the cascade mode and the soft momentum dependent equation of state mode of UrQMD model. Calculations are shown by the lines. Experimental data taken from the STAR Collaboration<sup>[23]</sup> are represented by the symbols.

fly away from the central region, so the influence of the average field becomes greater and greater.

## B. Average transverse momentum distributions

Fig. 7 show the  $\langle p_T \rangle$  as a function of  $\langle N_{part} \rangle$  at midrapidity ( $|y| < 0.1$ ) of  $\pi^+$ ,  $k^+$  and  $p$  for U+U collisions at  $\sqrt{s_{NN}}=193$  GeV. The black diamonds are the results calculated from the UrQMD model, and the red solid circles are the experimental data<sup>[23]</sup>. It is found that the experimental results can be described within the tolerance of error. The values of  $\langle p_T \rangle$  increase slowly with the decrease of collision centrality, and they are listed in Table I.

## C. Particle yields

Fig. 8 show the  $dN/dy$  as a function of  $\langle N_{part} \rangle$  at midrapidity ( $|y| < 0.1$ ) of  $\pi^+$ ,  $k^+$ ,  $p$  and  $\bar{p}$  in U+U collisions at  $\sqrt{s_{NN}}=193$  GeV. The black diamonds are the results calculated

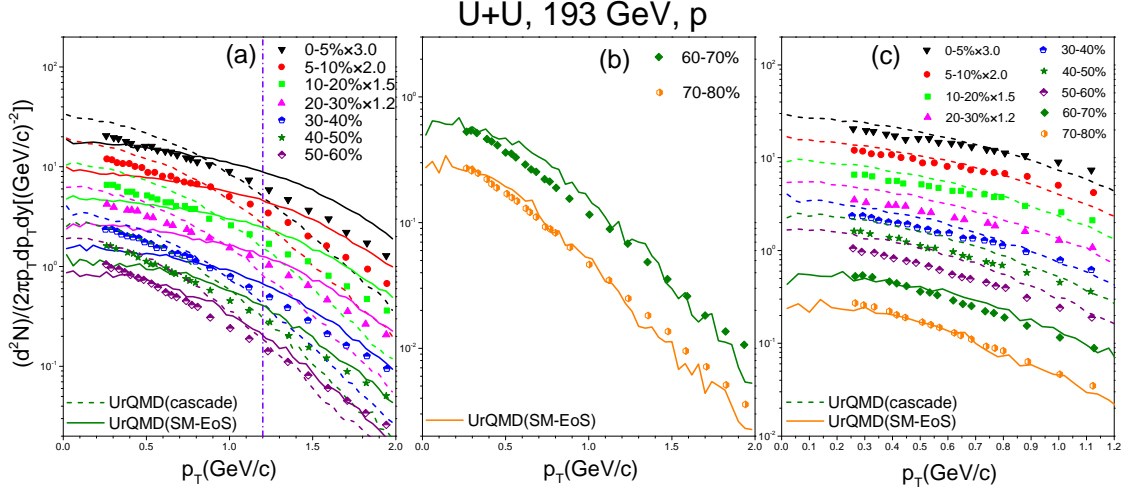


FIG. 5: Transverse momentum spectra of  $p$  are calculated at midrapidity ( $|y| < 0.1$ ) in U+U collisions at  $\sqrt{s_{NN}}=193$  GeV for 0–5%, 5–10%, 10–20%, 20–30%, 30–40%, 40–50%, 50–60%, 60–70% and 70–80% centralities from the cascade mode and the soft momentum dependent equation of state mode of UrQMD model. Calculations are shown by the lines. Experimental data taken from the STAR Collaboration<sup>[23]</sup> are represented by the symbols.

TABLE I: Values of  $\langle p_T \rangle$  in GeV/c within midrapidity ( $|y| < 0.1$ ) of  $\pi^+$ ,  $\pi^-$ ,  $k^+$ ,  $k^-$ ,  $p$  and  $\bar{p}$  for U+U collisions at  $\sqrt{s_{NN}}=193$  GeV using the UrQMD model.

Centrality	$\pi^+$	$\pi^-$	$k^+$	$k^-$	$p$	$\bar{p}$
0-5%	$0.454 \pm 0.092$	$0.454 \pm 0.093$	$0.668 \pm 0.037$	$0.667 \pm 0.019$	$0.985 \pm 0.028$	$1.039 \pm 0.020$
5-10%	$0.447 \pm 0.084$	$0.447 \pm 0.085$	$0.652 \pm 0.033$	$0.655 \pm 0.032$	$0.962 \pm 0.025$	$1.014 \pm 0.018$
10-20%	$0.438 \pm 0.073$	$0.438 \pm 0.073$	$0.637 \pm 0.029$	$0.636 \pm 0.027$	$0.934 \pm 0.022$	$0.982 \pm 0.016$
20-30%	$0.426 \pm 0.064$	$0.426 \pm 0.065$	$0.613 \pm 0.026$	$0.611 \pm 0.043$	$0.816 \pm 0.019$	$1.036 \pm 0.018$
30-40%	$0.414 \pm 0.049$	$0.414 \pm 0.049$	$0.586 \pm 0.019$	$0.584 \pm 0.018$	$0.849 \pm 0.015$	$0.882 \pm 0.011$
40-50%	$0.401 \pm 0.039$	$0.402 \pm 0.039$	$0.559 \pm 0.015$	$0.557 \pm 0.014$	$0.803 \pm 0.012$	$0.830 \pm 0.009$
50-60%	$0.393 \pm 0.031$	$0.393 \pm 0.031$	$0.535 \pm 0.012$	$0.536 \pm 0.011$	$0.745 \pm 0.009$	$0.764 \pm 0.007$
60-70%	$0.419 \pm 0.020$	$0.416 \pm 0.021$	$0.555 \pm 0.008$	$0.548 \pm 0.007$	$0.766 \pm 0.005$	$0.793 \pm 0.005$
70-80%	$0.408 \pm 0.012$	$0.409 \pm 0.013$	$0.530 \pm 0.005$	$0.526 \pm 0.005$	$0.708 \pm 0.003$	$0.730 \pm 0.003$

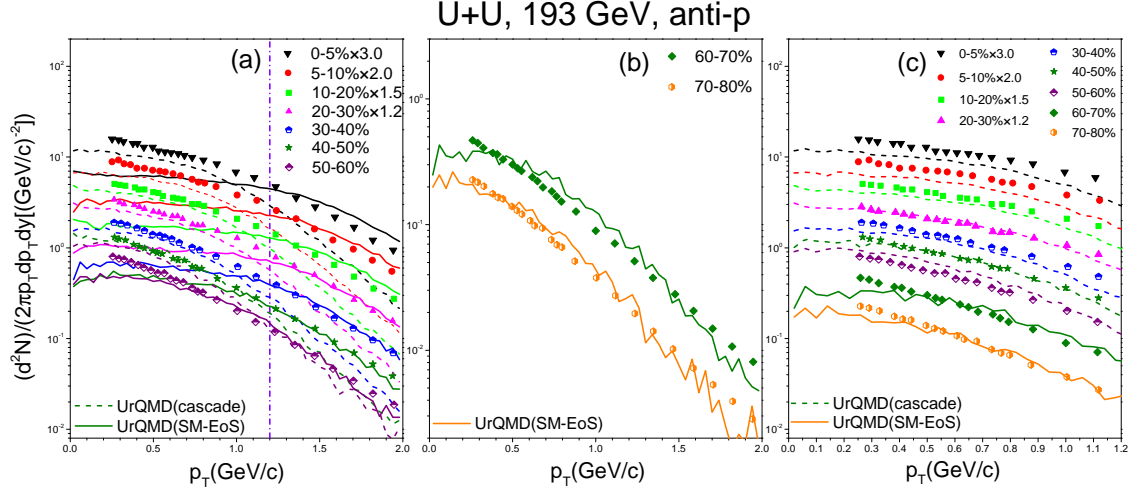


FIG. 6: Transverse momentum spectra of  $\bar{p}$  are calculated at midrapidity ( $|y| < 0.1$ ) in U+U collisions at  $\sqrt{s_{NN}}=193$  GeV for 0–5%, 5–10%, 10–20%, 20–30%, 30–40%, 40–50%, 50–60%, 60–70% and 70–80% centralities from the cascade mode and the soft momentum dependent equation of state mode of UrQMD model. Calculations are shown by the lines. Experimental data taken from the STAR Collaboration<sup>[23]</sup> are represented by the symbols.

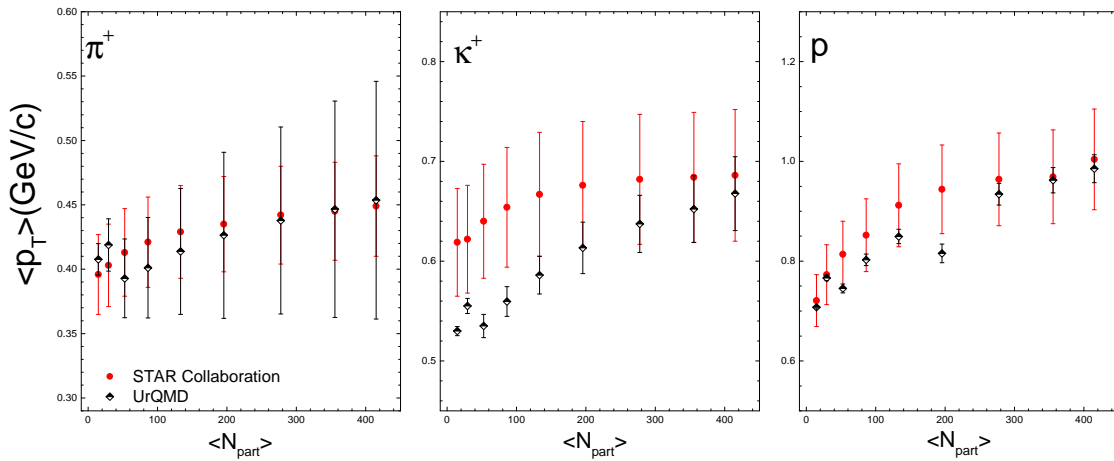


FIG. 7:  $\langle p_T \rangle$  as a function of  $\langle N_{part} \rangle$  at midrapidity ( $|y| < 0.1$ ) of  $\pi^+$ ,  $k^+$  and  $p$  for U+U collisions at  $\sqrt{s_{NN}}=193$  GeV. The red solid circles represent experimental data taken from the STAR Collaboration<sup>[23]</sup>. The black diamonds are the calculation using UrQMD model.

from the UrQMD model, and the red solid circles are the experimental data <sup>[23]</sup>. The values of  $dN/dy$  increase slowly with the decrease of collision centrality, and they are listed in Table II. It can be found that the theoretical results of  $k^+$ ,  $p$  and  $\bar{p}$  are in good agreement with the experimental data within the allowable error range, except that the  $\pi^+$  mesons of peripheral collision deviate greatly from the experimental solution. This is because  $\pi$  mesons are produced by nucleon-nucleon interaction, nucleon resonance states and baryon intermediate states decay. The nucleon resonance states and baryon intermediate states have great influence on the yield of  $\pi$  mesons. In the peripheral collision, these secondary effects are more full and more  $\pi$  mesons are produced.

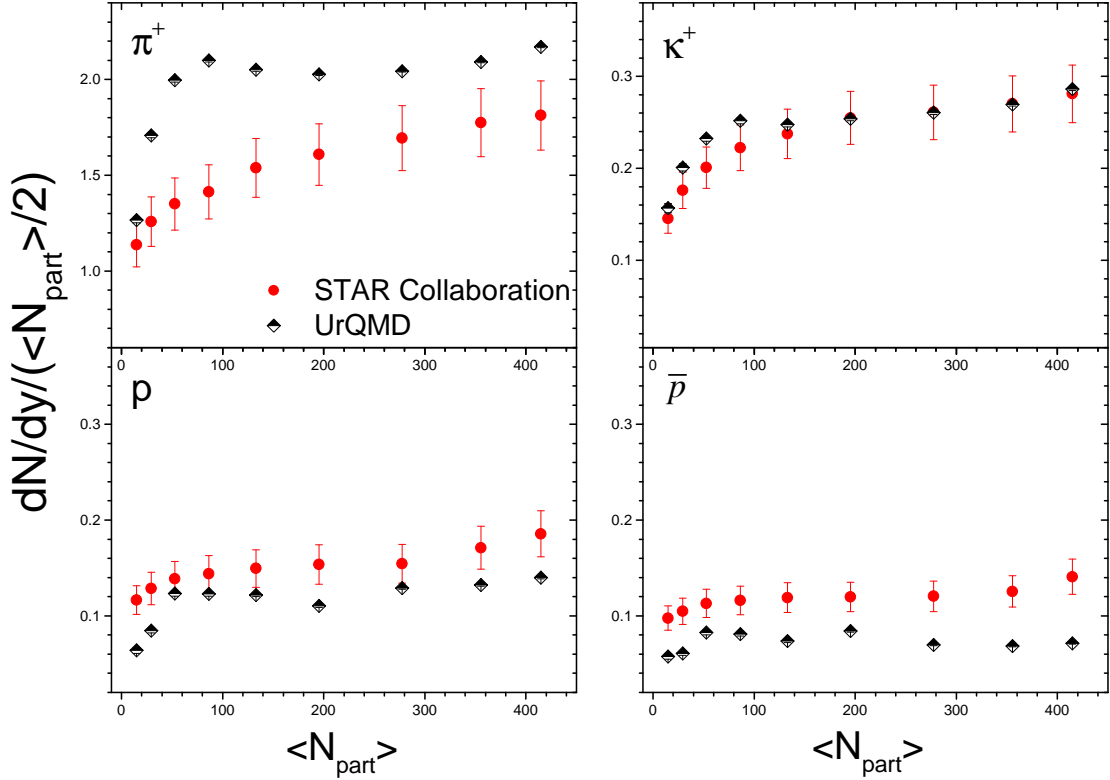


FIG. 8:  $dN/dy$  by  $\langle N_{part} \rangle / 2$  as a function of  $\langle N_{part} \rangle$  at midrapidity ( $|y| < 0.1$ ) of  $\pi^+$ ,  $K^+$ ,  $p$  and  $\bar{p}$  for U+U collisions at  $\sqrt{s_{NN}} = 193$  GeV. The red solid circles represent experimental data taken from the STAR Collaboration <sup>[23]</sup>. The black diamonds are the calculation using UrQMD model.

TABLE II: Values of  $dN/dy$  within midrapidity ( $|y| < 0.1$ ) of  $\pi^+$ ,  $\pi^-$ ,  $k^+$ ,  $k^-$ ,  $p$  and  $\bar{p}$  for U+U collisions at  $\sqrt{s_{NN}}=193$  GeV using the UrQMD model.

Centrality	$\pi^+$	$\pi^-$	$k^+$	$k^-$	$p$	$\bar{p}$
0-5%	$500.23 \pm 0.98$	$502.87 \pm 0.98$	$66.75 \pm 0.38$	$59.97 \pm 0.36$	$33.37 \pm 0.29$	$16.97 \pm 0.20$
5-10%	$412.81 \pm 0.89$	$415.42 \pm 0.89$	$53.76 \pm 0.34$	$48.97 \pm 0.33$	$27.04 \pm 0.26$	$14.02 \pm 0.19$
10-20%	$315.00 \pm 0.77$	$317.56 \pm 0.77$	$40.62 \pm 0.29$	$36.73 \pm 0.28$	$20.59 \pm 0.22$	$11.13 \pm 0.17$
20-30%	$220.00 \pm 0.64$	$222.89 \pm 0.64$	$27.89 \pm 0.24$	$25.28 \pm 0.23$	$12.40 \pm 0.17$	$9.47 \pm 0.16$
30-40%	$535.00 \pm 1.40$	$540.45 \pm 1.41$	$18.52 \pm 0.19$	$17.35 \pm 0.19$	$9.32 \pm 0.15$	$5.63 \pm 0.12$
40-50%	$100.53 \pm 0.41$	$101.35 \pm 0.42$	$12.19 \pm 0.15$	$10.98 \pm 0.14$	$6.09 \pm 0.12$	$4.01 \pm 0.10$
50-60%	$58.34 \pm 0.27$	$61.83 \pm 0.28$	$6.87 \pm 0.09$	$6.78 \pm 0.09$	$3.73 \pm 0.09$	$2.50 \pm 0.07$
60-70%	$27.89 \pm 0.19$	$29.51 \pm 0.19$	$3.32 \pm 0.06$	$3.29 \pm 0.06$	$1.43 \pm 0.04$	$1.03 \pm 0.04$
70-80%	$10.34 \pm 0.11$	$11.07 \pm 0.12$	$1.29 \pm 0.04$	$1.18 \pm 0.04$	$0.54 \pm 0.03$	$0.49 \pm 0.02$

#### D. Particle ratios

Fig. 9 show  $\pi^-/\pi^+$ ,  $k^-/k^+$  and  $\bar{p}/p$  as a function of  $\langle N_{part} \rangle$  at midrapidity ( $|y| < 0.1$ ) for U+U collisions at  $\sqrt{s_{NN}}=193$  GeV. The black diamonds are the results calculated from the UrQMD model, and the red solid circles are the experimental data <sup>[23]</sup>. It is found that the experimental results can be described within the tolerance of error. For  $\pi$  and  $k$ , the yield ratios are all approximately constant and near unity. This shows that positive and negative mesons are produced in pairs. For the  $\bar{p}/p$ , the collision from edge to center shows a slight downward trend. This shows that the more central the collision, the stronger the blocking effect on the proton.

#### IV. SUMMARY AND OUTLOOK

In summary, we have presented the transverse momentum spectra of  $\pi^\pm$ ,  $k^\pm$  and  $p(\bar{p})$  in midrapidity ( $|y| < 0.1$ ) for nine centrality classes : 0 – 5%, 5 – 10%, 10 – 20%, 20 – 30%, 30 – 40%, 40 – 50%, 50 – 60%, 60 – 70% and 70 – 80% in U+U collisions at  $\sqrt{s_{NN}}=193$  GeV. Other extracted observables from  $p_T$  spectra such as average transverse momentum ( $\langle p_T \rangle$ ), particle yields ( $dN/dy$ ) and particle ratios are also shown as functions of collision

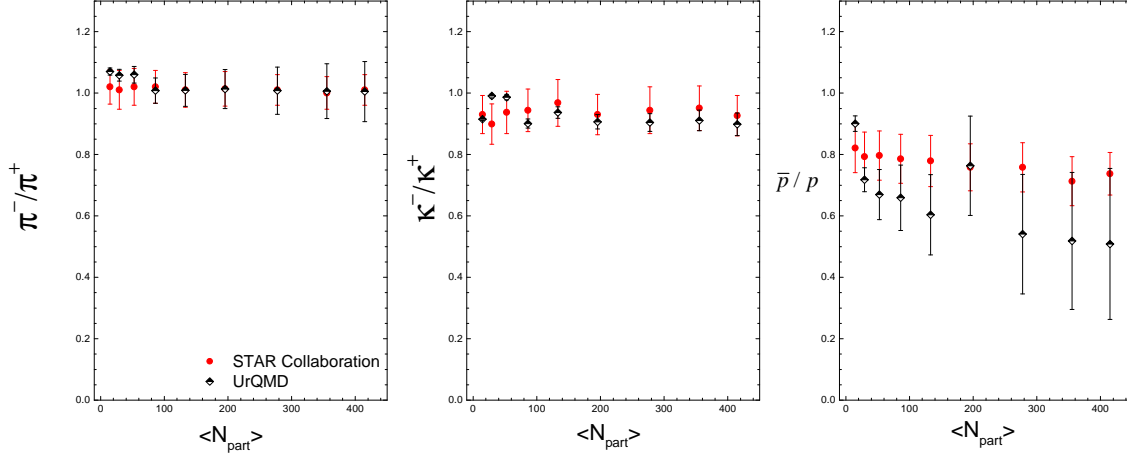


FIG. 9:  $\pi^-/\pi^+$ ,  $k^-/k^+$  and  $\bar{p}/p$  as a function of  $\langle N_{part} \rangle$  at midrapidity ( $|y| < 0.1$ ) for U+U collisions at  $\sqrt{s_{NN}}=193$  GeV. Experimental data taken from the STAR Collaboration<sup>[23]</sup> are represented by the red solid circles. The black diamonds are the calculation using UrQMD model.

centrality. We analyzed the experimental results from the STAR Collaboration<sup>[23]</sup> using the UrQMD model and found that the U+U collision process is segmented<sup>[35]</sup>, mainly because the U nucleus is the largest deformation nucleus. Due to its non-spherical symmetry, when the U+U collides along different directions, the central high-density material formed in the collision process will have different compression rates and lifetimes. Before the collision centrality is 50 – 60%, the experimental data are described well using cascade mode when the  $p_T < 1.2\text{GeV}/c$ . The results are in good agreement with the experimental data using the SM-EoS mode at  $p_T > 1.2\text{GeV}/c$ . For the case of 60 – 80% centrality, the SM-EoS mode describes the data better. Anti-particle to particle yield ratios indicating pair production is the dominant mechanism of particle production at RHIC energy. In the follow-up study, we will focus on the influence of the deformation of the U nucleus on the yield of particles at the final state of the collision.

### Conflict of Interests

The authors declare that there is no conflict of interests regarding the publication of this paper.

## Acknowledgements

We are grateful to the C3S2 computing center in Huzhou University for calculation support. This study used computational resources provided by Institute of Marine Drugs, Guangxi University of Chinese Medicine and the special Fund for Hundred Talents Program for Universities in Guangxi (Gui2019-71). The authors acknowledge the Beijing Super Cloud Computing Center (BSCC) for providing HPC resources that have contributed to the research results reported within this paper. URL: <http://www.blsc.cn/> This work was supported by the Fund for Less Developed Regions of the National Natural Science Foundation of China under Grant No.12365017, the Natural Science Foundation of Guangxi Zhuangzu Autonomous Region of China under Grant No. 2021GXNSFAA196052, the Introduction of Doctoral Starting Funds of Scientific Research of Guangxi University of Chinese Medicine under Grant No.2018BS024, and the Open Project of Guangxi Key Laboratory of Nuclear Physics and Nuclear Technology, No. NLK2020-03.

- 
- [1] C. Alt *et al.* [NA49 Collaboration], “Energy dependence of  $\Lambda$  and  $\Xi$  production in central Pb+Pb collisions at 20A, 30A, 40A, 80A, and 158A GeV measured at the CERN Super Proton Synchrotron,” *Physical Review C*, vol. 78, no. 3, Article ID 034918, 2008.
  - [2] J. X. Sun, F. H. Liu and E. Q. Wang, “Pseudorapidity Distributions of Charged Particles and Contributions of Leading Nucleons in Cu-Cu Collisions at High Energies,” *Chinese Physics Letters*, vol. 27, no. 3, Article ID 032503, 2010.
  - [3] E. Q. Wang, F. H. Liu, M. A. Rahim, S. Fakhraddin, J. X. Sun, “Singly and Doubly Charged Projectile Fragments in Nucleus-Emulsion Collisions at Dubna Energy in the Framework of the Multi-Source Model,” *Chinese Physics Letters*, vol. 28, no. 8, Article ID 082501, 2011.
  - [4] B. C. Li, and M. Huang, “Strongly coupled matter near phase transition,” *Journal of Physics G-Nuclear and Particle Physics*, vol. 36, Article ID 064062, 2009.
  - [5] F. H. Liu, “Anisotropic emission of charged mesons and structure characteristic of emission source in heavy ion collisions at 1–2A GeV,” *Chinese Physics B*, vol. 17, no. 3, pp. 883-895, 2008.
  - [6] M. I. Abdulhamid, *et al.* [STAR Collaboration], “Measurement of electrons from open heavy-flavor hadron decays in Au+Au collisions at  $\sqrt{s_{NN}} = 200$  GeV with the STAR detector,” *J. High Energ. Phys.*, vol. 2023, Article number 176, 2023.
  - [7] J. Adam, *et al.* [STAR Collaboration], “Beam-energy dependence of the directed flow of deuterons in Au+Au collisions,” *Phys. Rev. C*, vol. 102, Article ID 044906, 2020.
  - [8] R. Arsenescu *et al.* [NA52 Collaboration], “An investigation of the antinuclei and nuclei production mechanism in Pb + Pb collisions at 158 A GeV,” *New Journal of Physics*, vol. 5, pp. 150, 2003.
  - [9] Q. F. Li, Y. J. Wang, X. B. Wang and C. W. Shen, “Helium-3 production from Pb+Pb collisions at SPS energies with the UrQMD model and the traditional coalescence afterburner,” *Science China: Physics, Mechanics and Astronomy*, vol. 59, no. 3, Article ID 632002, 2016.
  - [10] H. L. Lao, H. R. Wei, F. H. Liu and Roy A. Lacey, “An evidence of mass-dependent differential kinetic freeze-out scenario observed in Pb-Pb collisions at 2.76 TeV,” *European Physical Journal A*, vol. 52, Article ID 203, 2016.
  - [11] S. Mrowczynski, P. Slon, “Hadron-Deuteron Correlations and Production of Light Nuclei in

- Relativistic Heavy-Ion Collisions,” <http://arxiv.org/abs/nucl-th/1904.08320v2>.
- [12] St. Mrowczynski, “Production of Light Nuclei in the Thermal and Coalescence Models,” *Acta Physica Polonica B*, vol. 48, pp. 707, 2017.
  - [13] St. Mrowczynski, “ ${}^4\text{He}$  versus  ${}^4\text{Li}$  and production of light nuclei in relativistic heavy-ion collisions,” *Modern Physics Letters A*, vol. 33, Article ID 1850142, 2018.
  - [14] P. Liu, J. H. Chen, Y. G. Ma and S. Zhang, “Production of light nuclei and hypernuclei at High Intensity Accelerator Facility energy region,” *Nuclear Science and Techniques*, vol. 28, Article ID 55, 2017.
  - [15] F. X. Liu, G. Chen, Z. L. Zhe, D. M. Zhou and Y. L. Xie, “Light (anti)nuclei production in Cu+Cu collisions at  $\sqrt{s_{NN}}=200$  GeV,” *European Physical Journal A*, vol. 55, Article ID 160, 2019.
  - [16] Y. Yuan, Q. F. Li, Z. X. Li, and F. H. Liu, “Transport model study of nuclear stopping in heavy-ion collisions over the energy range from 0.09A to 160A GeV,” *Physical Review C*, vol. 81, Article ID 034913, 2010.
  - [17] Y. Yuan, “Study of Production of (Anti-)deuteron Observed in Au+Au Collisions at  $\sqrt{s_{NN}}=14.5, 62.4$ , and 200 GeV,” *Advances in High Energy Physics*, vol. 2021, Article ID 9305605, 2021.
  - [18] P. C. Li, Y. J. Wang, Q. F. Li, H. F. Zhang, “Accessing the in-medium effects on nucleon-nucleon elastic cross section with collective flows and nuclear stopping,” *Physics Letters B*, vol. 828, Article ID 137019, 2022.
  - [19] Y. Yuan, Z. Q. Huang, X. F. Zhang, X. Z. Wei, “Transport model study of transverse momentum distributions of (anti-)deuterons production in Au+Au collisions at  $\sqrt{s_{NN}}=14.5, 62.4$ , and 200 GeV,” *Frontiers in Physics*, vol. 10, Article ID 971407, 2022.
  - [20] B. C. Li, Y. Y. Fu, L. L. Wang, F. H. Liu, “Dependence of elliptic flows on transverse momentum and number of participants in AuAu collisions at 200 GeV,” *Journal of Physics G-Nuclear and Particle Physics*, vol. 40, Article ID 025104, 2013.
  - [21] Y. H. Chen, F. H. Liu and Edward K. Sarkisyan-Grinbaum, “Event patterns from negative pion spectra in proton-proton and nucleus-nucleus collisions at SPS,” *Chinese Physics C*, vol. 42, no. 10, Article ID 104102, 2018.
  - [22] M. S. Abdallah, *et al.* [STAR Collaboration], “Azimuthal anisotropy measurement of (multi)strange hadrons in Au+Au collisions at  $\sqrt{s_{NN}}=54.4$  GeV,” *Physical Review C*, vol.

- 107, Article ID 024912, 2023.
- [23] M. S. Abdallah, *et al.* [STAR Collaboration], “Pion, kaon, and (anti) proton production in U+U collisions at  $\sqrt{s_{NN}}=193$  GeV measured with the STAR detector” *Physical Review C*, vol. 107, Article ID 024901, 2023.
  - [24] H. Petersen, M. Bleicher, S. A. Bass and H. Stocker, “UrQMD-2.3 - Changes and Comparisons,” <http://arxiv.org/abs/0805.0567>.
  - [25] B. Andersson, G. Gustafson and B. Nilsson-Almqvist, “A Model For Low P(T) Hadronic Reactions, With Generalizations To Hadron-Nucleus And Nucleus-Nucleus Collisions,” *Nuclear Physics B*, vol. 281, no. 1-2, pp. 289-309, 1987.
  - [26] B. Nilsson-Almqvist and E. Stenlund, “Interactions Between Hadrons And Nuclei: The Lund Monte Carlo, Fritiof Version 1.6,” *Computer Physics Communications*, vol. 43, no. 3, pp. 387-397, 1987.
  - [27] T. Sjostrand, “High-energy physics event generation with PYTHIA 5.7 and JETSET 7.4,” *Computer Physics Communications*, vol. 82, no. 1, pp. 74-89, 1994.
  - [28] S. A. Bass, M. Belkacem, M. Bleicher, M. Brandstetter, L. Bravina, C. Ernst, L. Gerland, M. Hofmann, S. Hofmann, J. Konopka, G. Mao, L. Neise, S. Soff, C. Spieles, H. Weber, L. A. Winckelmann, H. Stocker and W. Greiner, “Microscopic models for ultrarelativistic heavy ion collisions,” *Progress in Particle and Nuclear Physics*, vol. 41, pp. 255-369, 1998.
  - [29] H. Petersen, Q. F. Li, X. L. Zhu and M. Bleicher, “Directed and elliptic flow in heavy-ion collisions from  $E_{beam} = 90$  MeV/nucleon to  $E_{c.m.} = 200$  GeV/nucleon,” *Physical Review C*, vol. 74, Article ID 064908, 2006.
  - [30] S. A. Bass, M. Belkacem, M. Bleicher, M. Brandstetter, L. Bravina, C. Ernst, L. Gerland, M. Hofmann, S. Hofmann, J. Konopka, G. Mao, L. Neise, S. Soff, C. Spieles, H. Weber, L. A. Winckelmann, H. Stocker and W. Greiner, “Microscopic models for ultrarelativistic heavy ion collisions,” *Progress in Particle and Nuclear Physics*, vol. 41, pp. 255-369, 1998.
  - [31] M. Bleicher, E. Zabrodin, C. Spieles, S. A. Bass, C. Ernst, S. Soff, L. Bravina, M. Belkacem, H. Weber, H. Stocker and W. Greiner, “Relativistic hadron hadron collisions in the ultrarelativistic quantum molecular dynamics model,” *Journal of Physics G: Nuclear and Particle Physics*, vol. 25, no. 9, pp. 1859-1896, 1999.
  - [32] S. A. Bass, C. Hartnack, H. Stoecker and W. Greiner, “Azimuthal correlations of pions in relativistic heavy ion collisions at 1GeV/nucleon,” *Physical Review C*, vol. 51, no. 6, pp.

- 3343-3356, 1995.
- [33] Q. F. Li, Z. X. Li, S. Soff, M. Bleicher and H. Stoecker, “Probing the equation of state with pions,” *Journal of Physics G: Nuclear and Particle Physics*, vol. 32, no. 2, pp. 151-164, 2006.
  - [34] Q. F. Li and M. Bleicher, “A model comparison of resonance lifetime modifications, a soft equation of state and non-Gaussian effects on  $\pi - \pi$  correlations at FAIR/AGS energies,” *Journal of Physics G: Nuclear and Particle Physics*, vol. 36, no. 1, Article ID 015111, 2009.
  - [35] K. J. Wu, X. F. Luo and F. Liu, “Simulation for Elliptic Flow of UU Collisions at CSR Energy Region in Lanzhou,” *High Energy Physics and Nuclear Physics*, vol. 31, no. 7, pp. 617-620, 2007.